Nanoscale

PAPER

View Article Online
View Journal

Cite this: DOI: 10.1039/c9nr10965j

From bulk crystallization of inorganic nanoparticles at the air/water interface: tunable organization and intense structural colors†

Jacopo Vialetto, ‡ Sergii Rudiuk, Mathieu Morel and Damien Baigl *

Received 30th December 2019,
Accepted 28th January 2020

DOI: 10.1039/c9nr10965j

rsc.li/nanoscale

The "flipping method" is a new straightforward way to both adsorb and organize microparticles at a liquid interface, with ultralow amounts of a surfactant and no other external forces than gravity. Here we demonstrate that it allows the adsorption of a variety of inorganic nanoparticles at an air/water interface, in an organized way, which is directly controlled by the surfactant concentration, ranging from amorphous to highly crystalline two-dimensional assemblies. With micromolar amounts of a conventional cationic surfactant (dodecyltrimethylammonium bromide, DTAB), nanoparticles of different compositions (silica, silver, and gold), sizes (down to 100 nm) and shapes (spheres and cubes) adsorb from the bulk and directly organize at the air/water interface, resulting in marked optical properties such as reflectivity or intense structural coloration.

Introduction

Two-dimensional (2D) materials made of colloidal particles, organized in a long-range ordered fashion, find several applications in science and technology.[1–4] Particularly, the fabrication of structures composed of nanometer-size building-blocks is an important goal in materials science due to their specific responses arising from collective interactions. For example, they can be used for the fabrication of sensors,[5] surfaces with desired wettability[6] and reflective responses,[7,8] and biomimetic materials,[9] or for lithographic techniques.[10] Among others, optical properties are an exciting feature of organized colloidal monolayers,[11,12] which can exhibit structural coloration originating from the interaction of the incident light with periodic variations in the refractive index. Due to their light processing properties, photonic crystals are extensively studied to control, diffract, transmit or amplify the incoming radiation.[13] A well-defined periodic arrangement is required for the desired interaction with light; therefore precise control over the particle positioning and order is of utmost importance. For this purpose, fluid interfaces are a useful tool as templates for the formation of self-assembled structures,[14] with particle monolayers that span over macroscopic dimensions, having an exceptionally high degree of positional order, up to single crystals of mm^2 size.[15] Typically, for the formation of ordered monolayers, particles are externally added to a liquid interface by means of spreading drops from a concentrated suspension in a volatile solvent.[16–18] Crystallization can be achieved by increasing the number of adsorbed particles by several additions of spread drops,[19] or by compressing the monolayer with moving barriers (as in a Langmuir trough).[20] As alternatives to these multi-step and multiphasic approaches, a few one-step methods for achieving particle assembly and crystallization on a liquid interface from their suspension in a direct and precisely controlled fashion have been studied. Surfactants were commonly used to promote particle adsorption on liquid interfaces by modifying their hydrophilic/hydrophobic character, which resulted however, in the absence of external forces,[21] in irreversible aggregation and formation of amorphous assemblies.[22–24] The presence of millimolar amounts of salt,[5,25] coverage of the water solution with a charged lipid layer,[26,27] and the addition of excess thiol ligands[28] have also been explored for complete particle adsorption. In addition, external energy (*i.e.*, emulsification,[8] centrifugation,[25] and evaporation[28]) had to be typically applied to favor particle-interface proximity. All of these approaches have offered great tools to create and study ordered arrays or disordered assemblies of nanoparticles at fluid interfaces but share a level of experimental complexity that we propose to challenge in this report. We thus looked for a highly robust and single-step method and opted for the "flipping method", a strategy we recently described to organize particles at the air/water interface.[29,30] This very simple method was shown to be

PASTEUR, Department of Chemistry, Ecole Normale Supérieure, PSL University, Sorbonne Université, CNRS, 75005 Paris, France. E-mail: damien.baigl@ens.fr

†Electronic supplementary information (ESI) available. See DOI: 10.1039/c9nr10965j

‡Current address: Laboratory for Soft Materials and Interfaces, Department of Materials, ETH Zürich, Zürich, Switzerland.

particularly efficient for organizing microparticles in the presence of ultralow amounts of a surfactant, using no other additional forces than gravity. Here, we characterized the performance of this method to both adsorb and organize nanoparticles at the air–water (a/w) interface, by analyzing nanoparticles of different sizes (100 nm–1 μm), shapes (spheres, cubes), and compositions ranging from silica to silver and gold. For all these particle types, we studied how surfactants controlled the nanoparticle adsorption and packing organization. Under appropriate conditions, highly crystalline two-dimensional assemblies displaying intense structural colors were obtained.

Results and discussion

So far, the "flipping method" has been mainly used to tune the organization of polystyrene (PS) spheres of a few micrometers in diameter.[29,30] Here, we first applied this method to explore how the organization of anionic microparticles of a different composition could be tuned by the addition of minute amounts of a cationic surfactant. Briefly, a suspension of silica particles (2.4 μm in diameter) in water (particle concentration C_p = 0.05 mg mL^{-1}) was placed in a narrow cylindric cell to form a concave a/w meniscus, flipped upside down to let particles reach the a/w interface, and flipped back to its initial position. Only adsorbed particles remained at the interface prior to accumulating at its center to form a dense patch of particles. The particle suspension was mixed with dodecyltrimethylammonium bromide (DTAB), a cationic surfactant with a critical micellar concentration (CMC) of 13.4 mM, not only to enable the particle adsorption but also to tune the interaction between adsorbed particles and therefore their organization. We varied the surfactant concentration (C_s) and found, in a way similar to negatively charged PS microparticles,[29] that the number of adsorbed particles dramatically increased when C_s switched from 0 (Fig. S1†) to ≥1 μM (Fig. 1). The primary role of the cationic surfactant at $C_s \approx 10^{-4} \times$ CMC was as follows. The surfactant was accumulated at the a/w interface, not to compete with[31,32] the adsorption of the anionic silica particles at the negatively charged a/w interface, but instead to promote it by decreasing the electrostatic

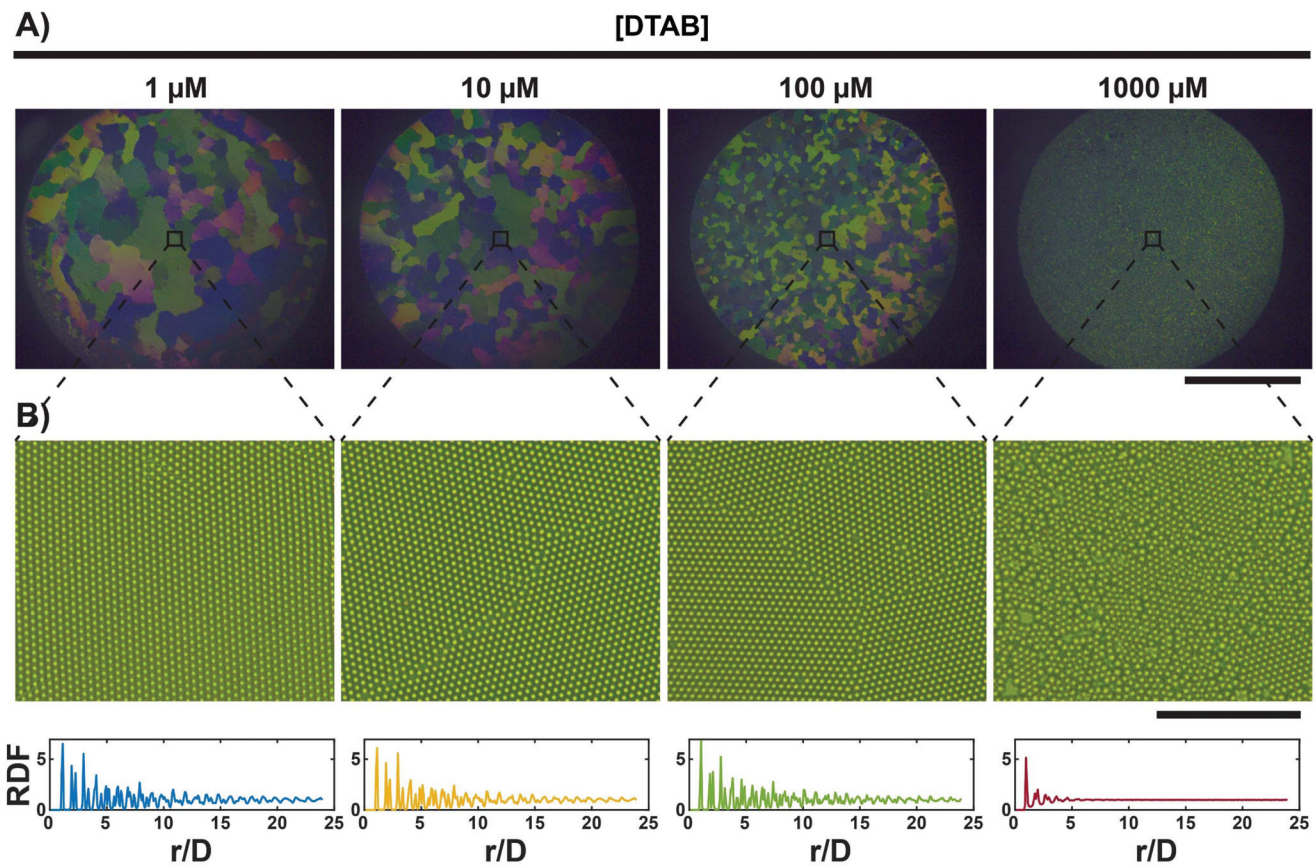

Fig. 1 Controlling the organization of silica microparticles adsorbed at the air/water interface. (A) Side-light reflection microscopy images of the particle assemblies at the a/w interface. The samples are illuminated with a white light source parallel to the liquid surface, and are composed of silica particles (diameter: 2.4 μm, C_p = 0.05 mg mL^{-1}) mixed with various concentrations of the cationic surfactant (dodecyltrimethylammonium bromide, DTAB). Scale bar: 1 mm. (B) High magnification brightfield transmission microscopy images of the center of the assemblies in A. Scale bar: 50 μm. Bottom row: radial distribution functions (RDFs) calculated in a larger window of the same images, of size 253 × 192 μm^2. D is the particle diameter, and r is the center-to-center distance.

adsorption barrier.[33] For $C_s \geq 1$ μM, a large number of adsorbed particles collectively deformed the interface to self-confine in its center according to the so-called sinking mechanism.[34] This resulted in the formation of large and dense assemblies of particles in an organized way, which depended on C_s (Fig. 1). When C_s ranged from 1 μM ($\approx 10^{-4} \times$ CMC) to 100 μM ($\approx 10^{-2} \times$ CMC), particles maintained most of their surface charge and formed highly organized structures of repulsive particles. This was not specific to DTAB as using a cationic surfactant with a different chemical structure but a similar CMC led to particle crystallization in the same range of C_s (Fig. S2†). At larger surfactant concentrations ($C_s \geq 1$ mM), particles became nearly neutralized by surfactants and formed amorphous assemblies.[22–24] For 1 μM $\leq C_s \leq$ 100 μM, the particle patch consisted of adjacent nearly defect-free monocrystalline domains separated by boundaries. Radial distribution function analyses allowed for a quantification of the positional order of the particles and indicated a well-ordered arrangement exceeding 20 particle diameters (Fig. 1B, bottom). A few differences with PS particles[29] should be noted: (i) when particles organized at low C_s, not only its center but also the whole patch crystallized and (ii) when the patch was amorphous at higher C_s, it did not form a loose gel-like assembly but remained dense. These differences were attributed to the higher density of silica compared to that of polystyrene, leading to a stronger collective deformation of the interface[34] and therefore a stronger self-confinement of the particles. Moreover, when the particle patches were irradiated with a white light source parallel to the a/w interface (Fig. S3†), polycrystalline structures exhibited bright structural coloration (Fig. 1A) due to the diffraction and constructive interference in the long-range ordered 2D crystals.[19,35] Each single-crystal domain was characterized by a distinct hue dependent on its orientation as well as on the curvature of the overall crystal, due to the deformation of the interface by the particles themselves through the collective sinking effect.[34] As a consequence, the size of each domain in the crystal structure could be visualized. We found that the domain size decreased with an increase in C_s, from larger domains, of around 0.3 mm^2 in the patch center, at C_s = 1 μM to smaller ones at C_s = 100 μM. Finally, a further increase in C_s caused the particles to assemble as disordered aggregates, with an almost complete loss of the structural coloration. These results show that the surfactant concentration tuned the organization of silica microparticle assemblies at the a/w interface and allowed the formation of highly organized 2D colloidal crystals with monocrystalline domains displaying specific structural colors and a size directly tunable by C_s.

We then explored how this principle could be extended to particles of much smaller dimensions. We thus used suspensions of silica nanoparticles at the same concentration (C_p = 0.05 mg mL^{-1}) but with different diameters (977 nm, 560 nm, 304 nm) and applied the "flipping method" in the presence of DTAB at low (C_s = 5 μM) and high (C_s = 1 mM) concentrations (Fig. 2). Compared to microparticles, the only difference was a much longer time in the "flipped" position (20 h *vs.* 2 h) to let

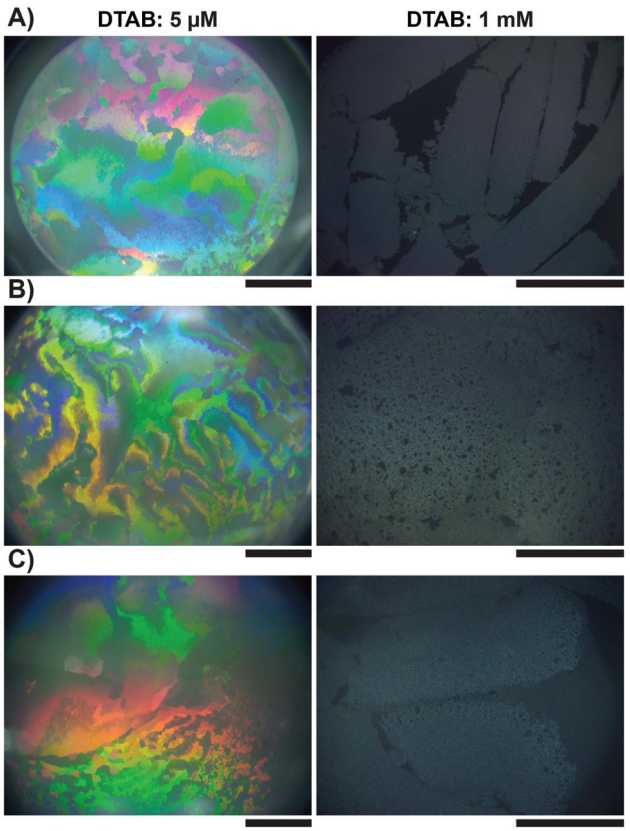

Fig. 2 Silica nanoparticles adsorbed at the air/water interface: surfactant-tunable organization and structural colors. Side-light reflection microscopy images of the particle assemblies at the a/w interface for samples containing silica particles (C_p = 0.05 mg mL^{-1}) having different diameters: 977 nm (A), 560 nm (B), and 304 nm (C). Left column: C_s = 5 μM; right column: C_s = 1 mM. Scale bars for all images: 1 mm.

the particles reach the interface (ESI, Experimental section†). First, side-light reflection microscopy revealed the presence of adsorbed materials at the water/air interface which was not observed in the absence of the surfactant. This confirmed the role of cationic surfactants to promote the adsorption of negatively charged particles at the a/w interface and showed that this method was still effective for silica nanoparticles regardless of their diameter. A strong dependence on the surfactant concentration was also observed. For C_s = 5 μM, intense structural colorations appeared on the whole patch for all particle diameters (Fig. 2, left). For the smallest particle size, successful crystallization was obtained for $C_p \geq 0.01$ mg mL^{-1} (Fig. S4†), showing that a minimal amount of particles was necessary to significantly deform the interface[34] and induce sufficient self-confinement. In contrast, for C_s = 1 mM, the patch was fragmented into large angular and whitish assemblies. By analogy with the observation made with microparticles (Fig. 1), we interpret the emergence of structural colors at low C_s as a result of the long-range organization of adsorbed nanoparticles at the a/w interface. The weak dependency on the particle size indicates that the structuration occurred

through the interstitial voids between ordered particles with similar arrangements and interparticle distances. Conversely, at a high C_s, the loss of structural coloration (Fig. 2, right) indicates the formation of disordered particle aggregates, which scattered the incoming white light in a random fashion. To confirm that the structural colors were actually due to the formation of an ordered monolayer of nanoparticles, we transferred the adsorbed particle assemblies onto a solid substrate for further characterization by scanning electron microscopy (SEM). This was carefully achieved by a slow evaporation of the water solution until the particle structure initially adsorbed on the water surface was deposited on a glass substrate (ESI, Experimental section and Fig. S5†). Note that the last step of evaporation was however non-homogeneous, causing the deposition of particles starting from the center toward the edge of the patch (Movie S1†). As a consequence, we expect this deposition method to induce an in-plane expansion stress which slightly perturbed the initial structure of the particle assembly. Representative images of the center of the particle deposits are displayed in Fig. 3. In the left, it shows the positional order achieved in the presence of a low amount of the surfactant

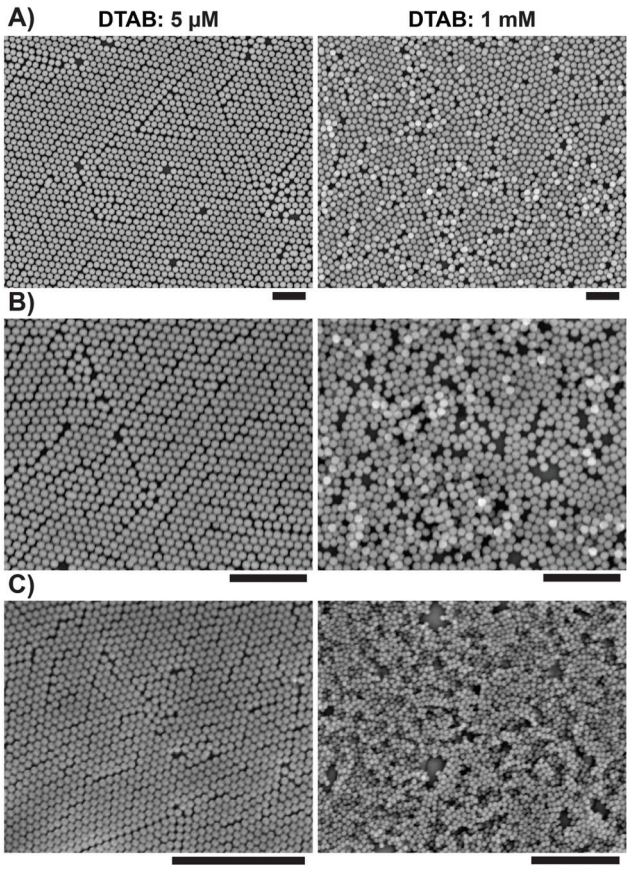

Fig. 3 Microstructure of the particle assemblies adsorbed at the air/water interface and then transferred to a glass substrate, as imaged using a scanning electron microscope (SEM). Samples composed of silica particles (C_p = 0.05 mg mL^{-1}) having different diameters: 977 nm (A), 560 nm (B), and 304 nm (C). Left column: C_s = 5 μM; right column: C_s = 1 mM. Scale bars for all images: 5 μm.

(C_s = 5 μM). Although few grain boundaries and vacancies probably generated during deposition were present, particles were forming hexagonally ordered, close-packed arrays regardless of their size. This indirectly confirmed that the nanoparticle assemblies at the a/w interface were 2D crystals. Conversely, for C_s = 1 mM, the particles on the solid substrates were disordered and arranged in a multi-layered fashion (Fig. 3, right), demonstrating that particle assemblies at the a/w interface were amorphous, and probably multi-layered, aggregates. These results show that, as for microparticles, the surfactant not only allowed the adsorption of silica nanoparticles at the a/w interface, but also controlled the way the nanoparticles organized once adsorbed. At C_s around 10^{-4} CMC, highly crystalline 2D assemblies with intense structural colors were obtained.

Finally, we investigated whether metal nanoparticles, commonly employed for the assembly of light processing 2D structures, such as photonic crystals[11] or liquid mirrors,[7] could be adsorbed at the a/w interface using our method. We thus applied it to nanoparticles having different compositions and shapes, namely silver nanocubes coated with poly (vinylpyrrolidone) (PVP), and gold nanospheres coated either with lipoic acid, or with poly(ethylene glycol) (PEG) with carboxylic acid terminations. All nanoparticles had a characteristic size of 100 nm. As in the previous cases, almost no particle adsorption at the a/w interface was observed in the absence of the surfactant (Fig. 4A and D, left and Fig. S6†). In the case of silver nanocubes, a small aggregate was occasionally observed in the center of the cell, but otherwise the interface was devoid of particles. In contrast, adding a very small amount of the surfactant (C_s = 5–10 μM) resulted in a complete coverage of the a/w interface with particles, as evidenced by reflection microscopy (Fig. 4A and D in the right, and Fig. S6†). We quantified the amount of light reflected by the interface with and without the added surfactant, by looking at the pixel intensity distribution of the reflection microscopy images (Fig. 4B and E). A shift of the histograms towards higher intensities indicated that the interface reflected the incoming white light more when the surfactant was used. This is further indication that the use of small amounts of the surfactant induced the adsorption of metal nanoparticles, thus allowing enhanced reflection of the incident light. To get better insight into the way particles organized at the a/w interface, we transferred the adsorbed particles on a solid substrate (Fig. S5†) and characterized the deposits by SEM (Fig. 4C and F). Both silver nanocubes and gold nanospheres displayed a local organization into μm-sized monolayered crystallites, coexisting with cracks attributed to the perturbation of the layer structure upon drying. Although we do not have direct access to the exact organization of the nanoparticles at the a/w interface, these results clearly demonstrate that the "flipping method" also allowed the adsorption of ordered monolayers of metal nanoparticles at the a/w interface and emphasize the striking role of micromolar amounts of cationic surfactants in controlling the behaviors of nanoparticles at the liquid interface.

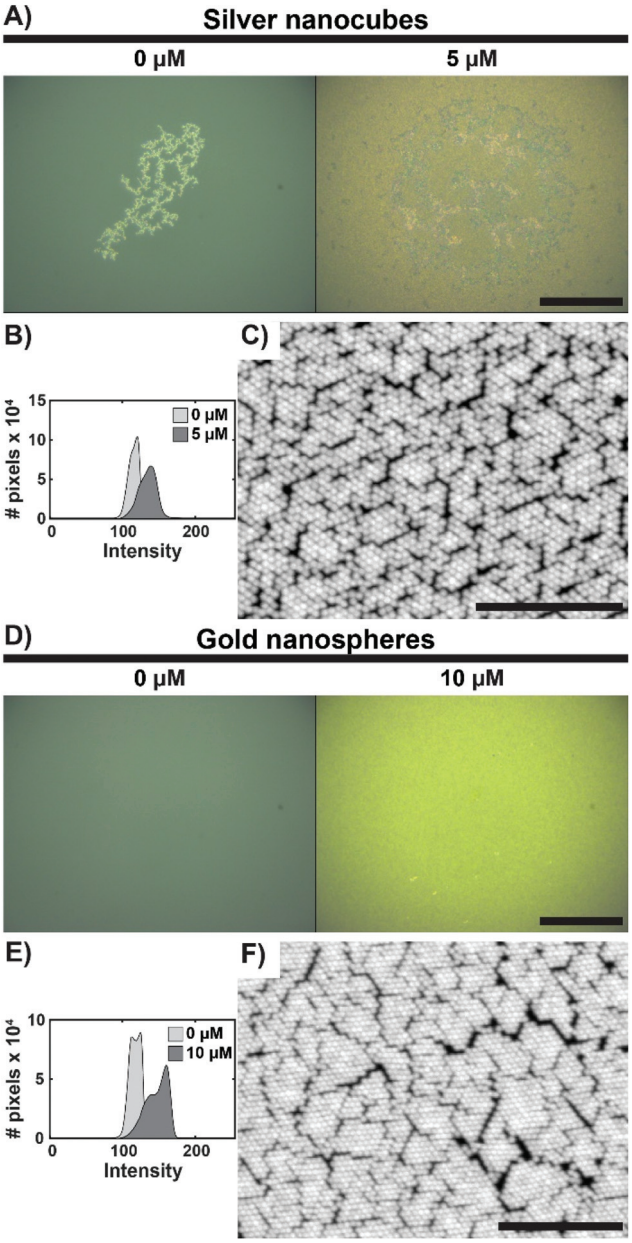

Fig. 4 Surfactant-induced adsorption of silver nanocubes (A–C) and gold nanospheres (D–F) at the air/water interface. (A and D) Direct reflection microscopy images of the air/water interface of samples containing C_p = 8 μg mL^{-1} of 100 nm silver cubes (A) or of 100 nm gold spheres (D), and various concentrations of DTAB. Scale bars: 100 μm. (B and E) Pixel intensity distribution of the images in (A and D), respectively. The light and dark grey curves correspond to the absence and addition of DTAB, showing an increase in light reflection from the interface in the presence of adsorbed particles. (C and F) SEM images of the microstructure of the particle assemblies adsorbed at the a/w interface and then transferred to a glass substrate. Scale bars: 2 μm.

Conclusions

We studied the behaviour of aqueous suspensions of anionic micro- and nanoparticles in a low cationic surfactant concentration regime (10^{-4} × CMC – 10^{-1} × CMC), focusing on particle adsorption at the a/w interface and subsequent assembly into crystalline or amorphous structures. Using the "flipping method", minute amounts of a conventional cationic surfactant (here DTAB) were shown to efficiently induce the adsorption of a variety of colloidal particles. The mechanism was found to be independent of the particle composition (silica, silver, and gold), size (down to ~100 nm), shape (spheres and cubes) and surface chemistry. The use of ultralow amounts of surfactants (10^{-4} × CMC – 10^{-2} × CMC) reproducibly resulted in ordered structures with marked optical signatures, such as light-reflective structures and polycrystalline assemblies displaying intense structural coloration. Our results emphasize the robustness of the "flipping method" to directly adsorb, from the bulk, anionic particles at the a/w interface in a controlled manner and its applicability to a variety of nanoparticle systems. Compared to conventional protocols, our method is advantageously simple, requiring nothing else than water as a solvent and a straightforward sample cell, in phase with the necessary development of "simple" material-fabrication techniques.[36] Gravity-based, it does not need any external compression step as particles spontaneously organize by self-confinement. Furthermore, with an organization directly controlled by small amounts of added surfactant, we suggest that using photosensitive[30] surfactants would be a straightforward way to make these assemblies photoswitchable and obtain their optical response, leading to new kinds of reconfigurable photonic devices.

Conflicts of interest

There are no conflicts to declare.

Acknowledgements

This work was supported by the Labex IPGG (ANR-10-LABX-31). We thank Yong Chen (Ecole Normale Supérieure) for providing us access to the scanning electron microscope. JV perfomed the experiments; all author analyzed the data; JV and DB wrote the paper with contribution from all authors.

Notes and references

1 O. D. Velev and S. Gupta, *Adv. Mater.*, 2009, **21**, 1897–1905.
2 R. McGorty, J. Fung, D. Kaz and V. N. Manoharan, *Mater. Today*, 2010, **13**, 34–42.
3 N. Vogel, M. Retsch, C.-A. Fustin, A. del Campo and U. Jonas, *Chem. Rev.*, 2015, **115**, 6265–6311.
4 V. Lotito and T. Zambelli, *Adv. Colloid Interface Sci.*, 2017, **246**, 217–274.
5 M. P. Cecchini, V. A. Turek, J. Paget, A. A. Kornyshev and J. B. Edel, *Nat. Mater.*, 2013, **12**, 165–171.
6 S. Portal-Marco, M. À. Vallvé, O. Arteaga, J. Ignés-Mullol, C. Corbella and E. Bertran, *Colloids Surf., A*, 2012, **401**, 38–47.

7 P.-P. Fang, S. Chen, H. Deng, M. D. Scanlon, F. Gumy, H. J. Lee, D. Momotenko, V. Amstutz, F. Cortés-Salazar, C. M. Pereira, Z. Yang and H. H. Girault, *ACS Nano*, 2013, **7**, 9241–9248.
8 Y. Xu, M. P. Konrad, W. W. Y. Lee, Z. Ye and S. E. J. Bell, *Nano Lett.*, 2016, **16**, 5255–5260.
9 M. Kolle, P. M. Salgard-Cunha, M. R. J. Scherer, F. Huang, P. Vukusic, S. Mahajan, J. J. Baumberg and U. Steiner, *Nat. Nanotechnol.*, 2010, **5**, 511–515.
10 L. Isa, K. Kumar, M. Müller, J. Grolig, M. Textor and E. Reimhult, *ACS Nano*, 2010, **4**, 5665–5670.
11 A. Tao, P. Sinsermsuksakul and P. Yang, *Nat. Nanotechnol.*, 2007, **2**, 435–440.
12 Y. H. Lee, W. Shi, H. K. Lee, R. Jiang, I. Y. Phang, Y. Cui, L. Isa, Y. Yang, J. Wang, S. Li and X. Y. Ling, *Nat. Commun.*, 2015, **6**, 6990.
13 G. von Freymann, V. Kitaev, B. V. Lotsch and G. A. Ozin, *Chem. Soc. Rev.*, 2013, **42**, 2528–2554.
14 M. Grzelczak, J. Vermant, E. M. Furst and L. M. Liz-Marzán, *ACS Nano*, 2010, **4**, 3591–3605.
15 E. Sirotkin, J. D. Apweiler and F. Y. Ogrin, *Langmuir*, 2010, **26**, 10677–10683.
16 R. Aveyard, J. H. Clint, D. Nees and V. N. Paunov, *Langmuir*, 2000, **16**, 1969–1979.
17 S. M. Weekes, F. Y. Ogrin, W. A. Murray and P. S. Keatley, *Langmuir*, 2007, **23**, 1057–1060.
18 J.-T. Zhang, L. Wang, D. N. Lamont, S. S. Velankar and S. A. Asher, *Angew. Chem., Int. Ed.*, 2012, **51**, 6117–6120.
19 N. Vogel, S. Goerres, K. Landfester and C. K. Weiss, *Macromol. Chem. Phys.*, 2011, **212**, 1719–1734.
20 N. Vogel, L. de Viguerie, U. Jonas, C. K. Weiss and K. Landfester, *Adv. Funct. Mater.*, 2011, **21**, 3064–3073.
21 K. P. Velikov, F. Durst and O. D. Velev, *Langmuir*, 1998, **14**, 1148–1155.
22 D. C. E. Calzolari, D. Pontoni, M. Deutsch, H. Reichert and J. Daillant, *Soft Matter*, 2012, **8**, 11478.
23 A. Maestro, E. Guzmán, E. Santini, F. Ravera, L. Liggieri, F. Ortega and R. G. Rubio, *Soft Matter*, 2012, **8**, 837–843.
24 M. Anyfantakis, Z. Geng, M. Morel, S. Rudiuk and D. Baigl, *Langmuir*, 2015, **31**, 4113–4120.
25 V. A. Turek, M. P. Cecchini, J. Paget, A. R. Kucernak, A. A. Kornyshev and J. B. Edel, *ACS Nano*, 2012, **6**, 7789–7799.
26 S. Srivastava, D. Nykypanchuk, M. Fukuto, J. D. Halverson, A. V. Tkachenko, K. G. Yager and O. Gang, *J. Am. Chem. Soc.*, 2014, **136**, 8323–8332.
27 S. Srivastava, D. Nykypanchuk, M. Fukuto and O. Gang, *ACS Nano*, 2014, **8**, 9857–9866.
28 T. P. Bigioni, X.-M. Lin, T. T. Nguyen, E. I. Corwin, T. A. Witten and H. M. Jaeger, *Nat. Mater.*, 2006, **5**, 265–270.
29 M. Anyfantakis, J. Vialetto, A. Best, G. K. Auernhammer, H.-J. Butt, B. P. Binks and D. Baigl, *Langmuir*, 2018, **34**, 15526–15536.
30 J. Vialetto, M. Anyfantakis, S. Rudiuk, M. Morel and D. Baigl, *Angew. Chem., Int. Ed.*, 2019, **58**, 9145–9149.
31 X. Hua, M. A. Bevan and J. Frechette, *Langmuir*, 2018, **34**, 4830–4842.
32 J. Smits, F. Vieira, B. Bisswurn, K. Rezwan and M. Maas, *Langmuir*, 2019, **35**, 11089–11098.
33 D. F. Williams and J. C. Berg, *J. Colloid Interface Sci.*, 1992, **152**, 218–229.
34 D.-G. Lee, P. Cicuta and D. Vella, *Soft Matter*, 2017, **13**, 212–221.
35 B. van Duffel, R. H. A. Ras, F. C. De Schryver and R. A. Schoonheydt, *J. Mater. Chem.*, 2001, **11**, 3333–3336.
36 X. Tian, K. R. Lind, B. Yuan, S. Shaw, O. Siemianowski and L. Cademartiri, *Adv. Mater.*, 2017, **29**, 1604681.

